www.czasopisma.pan.pl PAN POLSKA AKADEMIA NAUK www.journals.pan.pl

A R C H I V E S O F M E T A L L U R G Y A N D M A T E R I A L S

Volume 60 2015 Issue 3

DOI: 10.1515/amm-2015-0369

H. PAUL*#, M. M. MISZCZYK*

DEFORMATION MICROSTRUCTURE AND TEXTURE TRANSFORMATIONS IN FCC METALS OF MEDIUM-TO-HIGH STACKING FAULT ENERGY: CRITICAL ROLE OF MICRO- AND MACRO-SCALE SHEAR BANDS

ZMIANY MIKROSTRUKTURALNE I TEKSTUROWE W ODKSZTAŁCONYCH METALACH O SIECI RSC O ŚREDNIEJ I WYSOKIEJ ENERGII BŁĘDU UŁOŻENIA: KRYTYCZNA ROLA MIKRO- I MAKRO-PASM ŚCINANIA

Microstructure and texture development in medium-to-high stacking fault energy face centred cubic metals were investigated in order to examine the role of lattice re-orientation on slip propagation across grain boundaries and to characterize the influence of micro- and macro-scale copper-type shear bands on textural changes at large deformations. Polycrystalline pure copper (fine - and coarse - grained) and fine-grained AA1050 alloy were deformed in plane strain compression at room temperature to form two sets of well-defined macroscopic shear bands. The deformation-induced sub-structures and local changes in crystallographic orientations were investigated mostly by scanning electron microscopy equipped with high resolution electron backscattered facility. In all the deformed grains within macro- shear bands a strong tendency to strain-induced re-orientation was observed. The flat, strongly deformed grains exhibited a deflection within narrow areas. The latter increased the layers' inclination with respect to ED and led to kink-type bands, which are the precursors of MSBs. The mechanism of macro- / micro-shear bands formation is strictly crystallographic since in all the areas of the sheared zone, the crystal lattice rotated such that one of the {111} slip planes became nearly parallel to the shear plane and the <011> direction became parallel to the direction of maximum shear. This strain-induced crystal lattice rotation led to the formation of specific macro- / micro-shear bands components that facilitated slip propagation across the grain boundaries without any visible variation in the slip direction.

Keywords: Shear bands, Texture, SEM/EBSD, Copper, AA1050 alloy, Plane strain compression

W pracy badano zmiany strukturalne i teksturowe w metalach o sieci regularnej ściennie centrowanej związane z lokalną re-orientacją sieci krystalicznej wynikającą z formowania się mikro- i makro- pasm ścinania. Analizowano polikrystaliczne próbki miedzi oraz aluminium o czystości technicznej (stop AA1050) odkształcane w temperaturze otoczenia w próbie nieswobodnego ściskania do zakresu odkształceń, w których następuje wyraźne uformowanie się dwóch rodzin makroskopowych pasm ścinania. W badaniach wykorzystano skaningowy mikroskop elektronowy wyposażony w system automatycznego pomiaru orientacji lokalnych. Zaobserwowano, że w ziarnach umiejscowionych w obszarze makroskopowych pasm ścinania występuje ściśle zdefiniowana tendencja rotacji sieci krystalicznej, w wyniku której jedna z płaszczyzn typu {111} przyjmuje położenie zbliżone do położenia płaszczyzny ścinania, a jeden z kierunków typu <110> (lub <112>) wykazuje tendencję do sytuowania się równolegle do kierunku ścinania. Obserwowana w obszarze wnętrza pasm ścinania rotacja prowadzi do uformowania się specyficznej (mikro)tekstury, która umożliwia propagację poślizgów poprzez granice ziaren bez 'istotnej' zmiany kierunku ścinania.

1. Introduction

It has been well known for decades that plastic deformation of metals is not homogeneous but concentrated in different kinds of inhomogeneities of plastic flow. Shear bands (SBs) or their compact clusters, called macroscopic shear bands (MSBs), are frequently observed examples of unstable behaviour of *fcc* metallic materials at large strains, e.g. [1-14]. However, their formation and development within the as-deformed structures and their influence on the overall texture evolution are still not completely understood [12-16]. In particular, there is still no agreement on the fundamental problem whether slip within SBs is crystallographic or non-crystallographic, i.e. whether or not the shears occur in *fcc* metals on {111}-type planes and along <110> – type directions , e.g. [6,8,17-19]. It is also unclear how the onset of unstable flow depends on the material history and how the internal texture of the SBs influences the global deformation texture?, e.g. [20-22]. However, there are also widely

* INSTITUTE OF METALLURGY AND MATERIALS SCIENCE, PAS, 25 REYMONTA STR., 30-059 KRAKÓW, POLAND

Corresponding author: h.paul@imim.pl

accepted facts. Those associated with shear banding in fcc single crystals can be summarized as follows. (*i*) Shear bands are not observed in microstructures dominated by equiaxed dislocation cells and near isotropic properties [22]. (*ii*) Shear banding is preceded by the formation of essentially planar obstacles to homogeneous dislocation glide [7-11,17-19]. (*iii*) Two groups of SBs can be distinguished according to the SFE. In metals with a low SFE, *brass-type SBs* can be readily observed after medium deformations, e.g. [2-19]. They develop within the microstructures characterized by thin twin-matrix lamellae. In metals of a medium-to-high SFE, *copper-type SBs* are formed against the background of band-like dislocation structures of elongated cells (micro-bands), e.g. [6-11]. (*iv*) Shear banding tends to become increasingly difficult in metals of very high SFE, and so have not always been observed in high purity aluminium [23].

In *fcc* polycrystals the orientation changes induced by shear banding have been studied by both X-ray diffraction, e.g. [24,25] and EBSD technique, e.g. [11,17-19]. However, in polycrystalline metals the situation can be quite complicated. In this case MSBs very often cross the grain boundaries without any significant change in shear direction. From the point of view of crystallography the requirement of slip propagation across grain boundaries leads to some basic questions about the mechanisms responsible for slip system organization along traces of the shear plane within differently oriented grains situated inside the sheared zone.

The opinion that SBs are *non-crystallographic* derives from macroscopic observations and the general considerations of the stability of the {112} <111> orientation (having a strong tendency to form SBs) at high strains [26, 27]. The concept of *crystallographic SBs* is based on the idea that the planar obstacles to dislocation glide are bent as an essential 'precursor' to shear banding. This concept, developed in a series of single crystals studies [8, 17-19, 22, 28-30] assumes that the local lattice re-orientation within narrow areas increases the activity of the previously low activity (or inactive) slip systems in the neighbouring matrix.

In this work, the microtexture development in pure polycrystalline copper and fine-grained AA1050 alloy have been investigated in order to characterize the influence of local lattice re-orientations within particular grains on slip propagation across the grain boundaries and the formation of macroscopically visible clusters of copper-type shear bands. Computer-automated electron backscattered diffraction (EBSD) is a particularly suitable method of investigating the phenomenon.

2. Experimental

Samples of fine- and coarse- grained copper (99.98%) were deformed in plane strain compression (PSC) and rolling to a thickness reduction of 70% and 80%, respectively. The microstructure of fine-grained copper consisted of nearly equiaxial grains with an average grain size of ~ 50 μm. The orientation distribution, determined by X-ray diffraction, revealed a relatively weak texture without any significant tendency for peak texture components. PSC tests performed in this work were twofold. During the first PSC test the samples were deformed continuously up to 70%, whereas during the second one the samples were deformed in two stages using markers to locate the MSBs. The initial sample was channel-die compressed 24%. Then, on the longitudinal ND-ED plane, three scratches along ED were made. ND, ED (|| RD) and TD denote the normal, extrusion (|| rolling) and transverse direction, respectively. The sample was further compressed up to ~50%, at which clearly defined MSBs were visible. Details of slip propagation across grain boundaries were analysed in polycrystalline copper which microstructure consisted of extremely large grains with an average grain size of ~500 μm.

Samples of AA1050 alloy were preliminary ECAP-processed using a 90° die with an outer corner radius of 5 mm and channel cross section of 10 × 10 mm^2. This gave a nominal (von Mises) effective strain of $\varepsilon_M = 1.1$ per pass. The samples were compressed along route C, i.e. the samples underwent a 180° rotation around the extrusion direction (ED) in consecutive passes (in each case, ED was parallel to RD). In the case of commercially pure Al, a very large amount of ECAP deformation can lead to dynamic recrystallization, as observed earlier for pure aluminium [31]. Therefore, the pre-deformation was limited to 6 passes (a microstructure free of recrystallized grains). The billet and the tooling were well-lubricated with MoS_2-containing grease. After each pass, the die was opened, and the sample was removed from the die, re-polished and subjected to the next pass. The initial structure of large flat grains was transformed during the ECAP processing into a structure of very fine-grains grouped in layers.

The ECAP processed samples were sectioned perpendicular to ED (i.e. along the ND-TD plane) in the centre of the billets. Cubic samples of 10×10×10 mm^3 were inserted into a channel-die for PSC at a punch speed of 0.5 mm / min. To reduce friction between specimen and the compression rig, a 50 μm thick Teflon^{TM} lubricant was used during testing. Cubic samples were deformed to logarithmic strains of ~0.3, by two-stage tests involving a change of the Teflon^{TM} ribbon. The ratio between the height and length of the test pieces was restored to 1 at the beginning of the second deformation step (by removing the extremities on the free surfaces). The surfaces were carefully marked so that the ED of the ECAP and plane strain compressed sample was parallel to the RD of the initial material (Fig. 1).

The deformation-induced dislocation structures and local changes in crystallographic orientations were investigated by SEM - JEOL JSM 6500F equipped with a field emission gun and facilities for electron backscattered diffraction (EBSD). To reveal the crystallographic contrast backscattered electrons operating at 20 kV were used. The microscope control, pattern acquisition and solution were carried out with the HKL Channel 5 system. For more global (i.e. sample) scale microstructure observations an optical microscopy was used on mechanically and chemically polished samples. Additionally, the texture variation in the global scale were analysed by X-ray diffraction from the as-received to final as-deformed states.

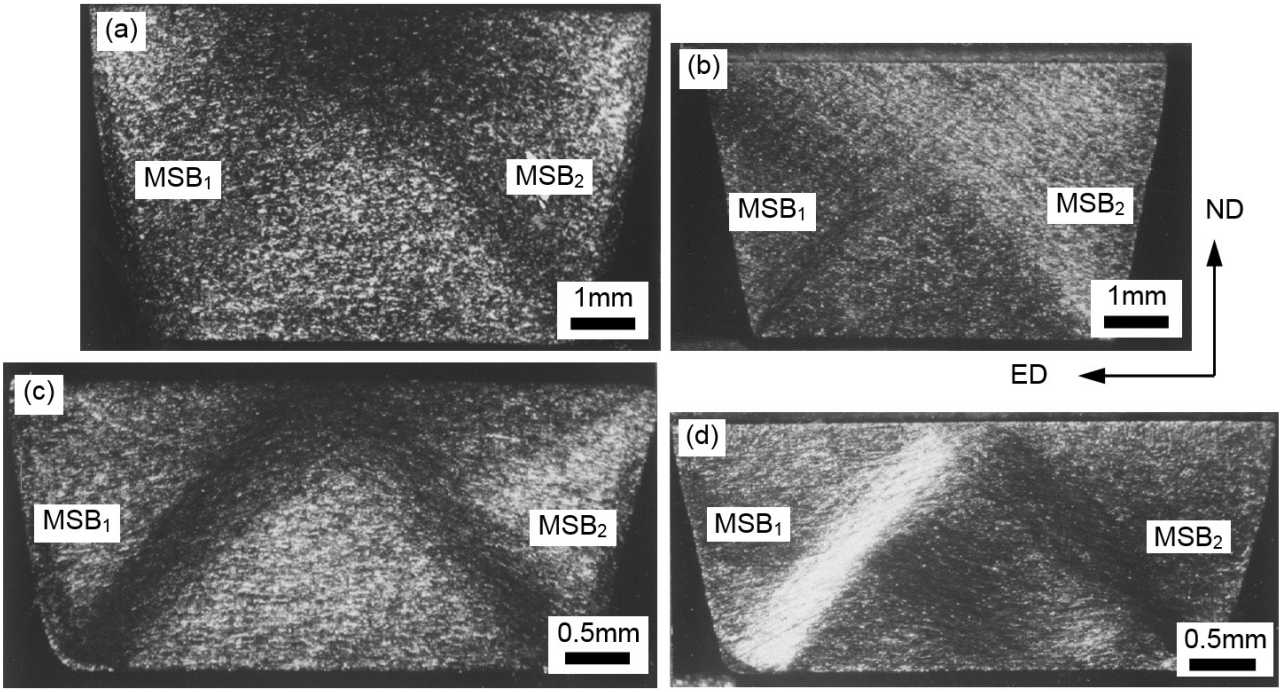

Fig. 1. Macroscopic shear bands developed in fine-grained copper. Samples deformed in channel die up to: (a) 40%, (b) 50%, (c) 60% and (d) 70%. Optical micrographs on longitudinal section, i.e. perpendicular to TD

3. Results

3.1. PSC of polycrystalline copper

3.1.1. Macroscopic changes at the sample scale

The structure of fine-grained copper in the reductions ranged between 40% and 70% illustrate the gradual tendency to macro-scale strain localization in two families of MSBs. Both families of MSBs operates in planes inclined at an angle of about 45°, which corresponds to the position of the plane of maximal shear stress, as presented in (Fig. 1). After the deformation to 50%, the MSBs were formed a characteristic V shaped set of two families (Fig. 1 and 2). The width of each set was 1.5-2 mm and they were positively and negatively inclined at ~45° to ED. The scratches made on the longitudinal plane (along ED) showed a well-defined rotation (Fig. 2), of opposite sign within each set of macro-shear bands. This rotation occurs with the increasing inclination of the line segments crossed by MSBs. The values of the rotation angles inside MSB_1 and MSB_2 attain ~ ±20° (Fig. 3). The inclination of the lines decreased outside the bands. Clearly the macroscopic rotation observed within both families of bands influences the crystal lattice rotations of grains situated within the MSB volumes.

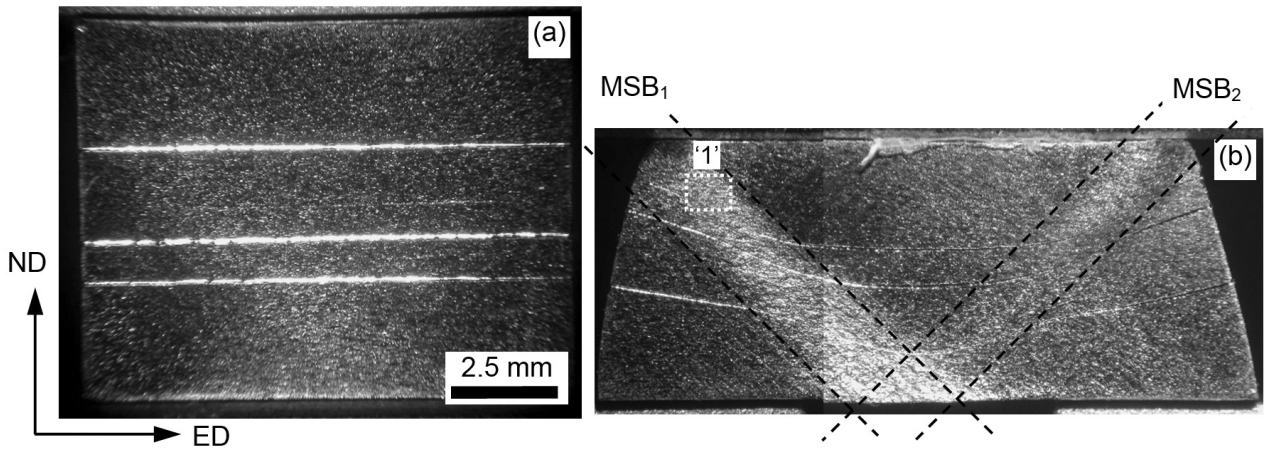

Fig. 2. MSBs formation and shear deformation in copper samples deformed in channel-die. (a) Initial position of scratches after 24% reduction. (b) Bending of the scratches within MSB_1 and MSB_2 after further 25% deformation up to a final 50% reduction. Optical micrographs on longitudinal (i.e. ND-ED) plane

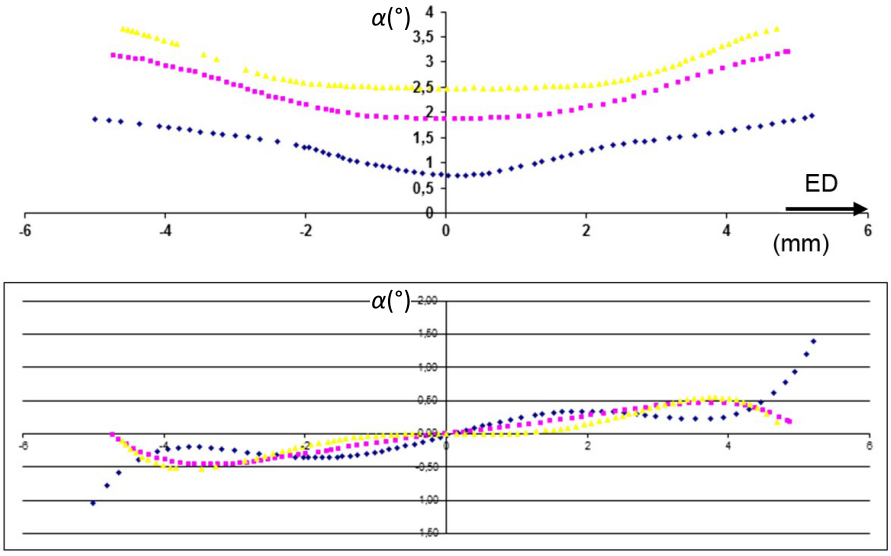

Fig. 3. (a) Changes in the inclination angle (α) of the scratches made on longitudinal plane and (b) values of tg(α) along ED for particular lines presented in (Fig. 2a). X axis is distance in mm. Sample deformed 50%

In coarse-grained copper, the traces of the grain boundaries revealed a well-defined rotation of opposite sign within each set of bands (Fig. 4a). The sense of this rotation is such as to increase the inclination of the layers with respect to ED.

Optical microscopy analysis that was more detailed showed that straight micro-bands inclined at ~45° to ED cross the kinked layers of flat grains placed inside the MSB_1 (Fig. 4b). The microstructure of macro-shear bands observed at TEM scale (Fig. 5) is composed of single micro-shear bands that are situated along the {111} planes (in each flat grain), as shown by the {111} pole figures.

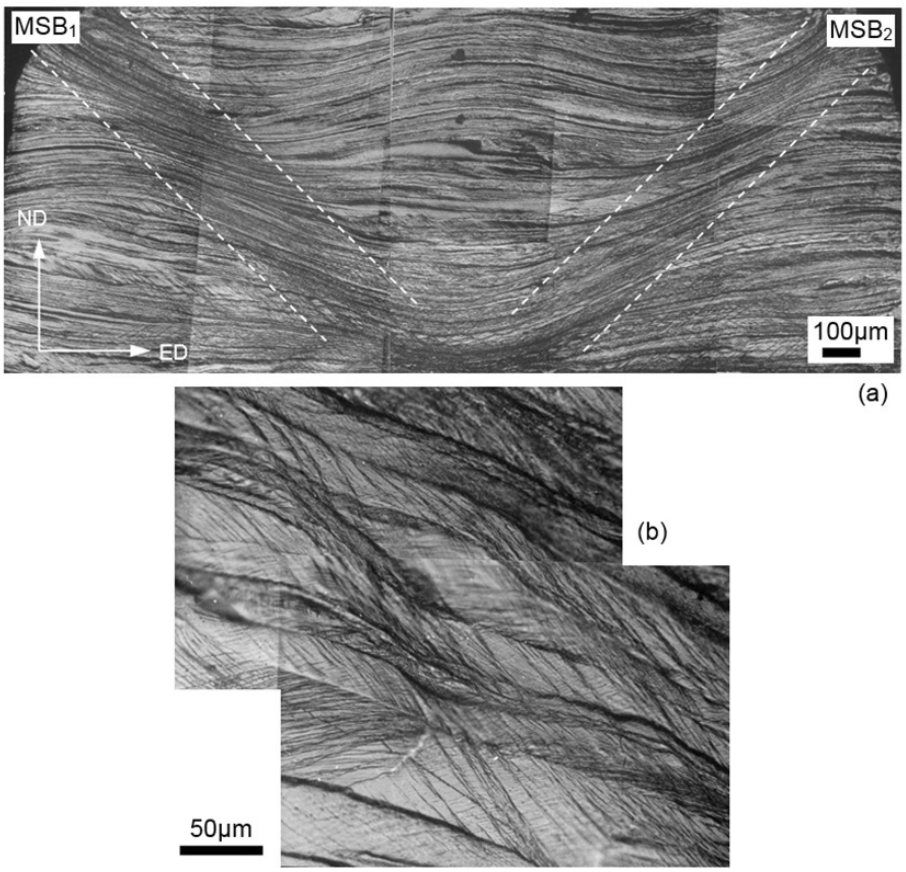

Fig. 4. Macro-shear bands formation in coarse-grained copper sample deformed 90% in channel-die. (a) Bending of flat grains within MSBs zones and (b) detail from (a) showing slips propagation across the neighbouring grains. Optical micrographs on longitudinal (i.e. ND-ED) plane

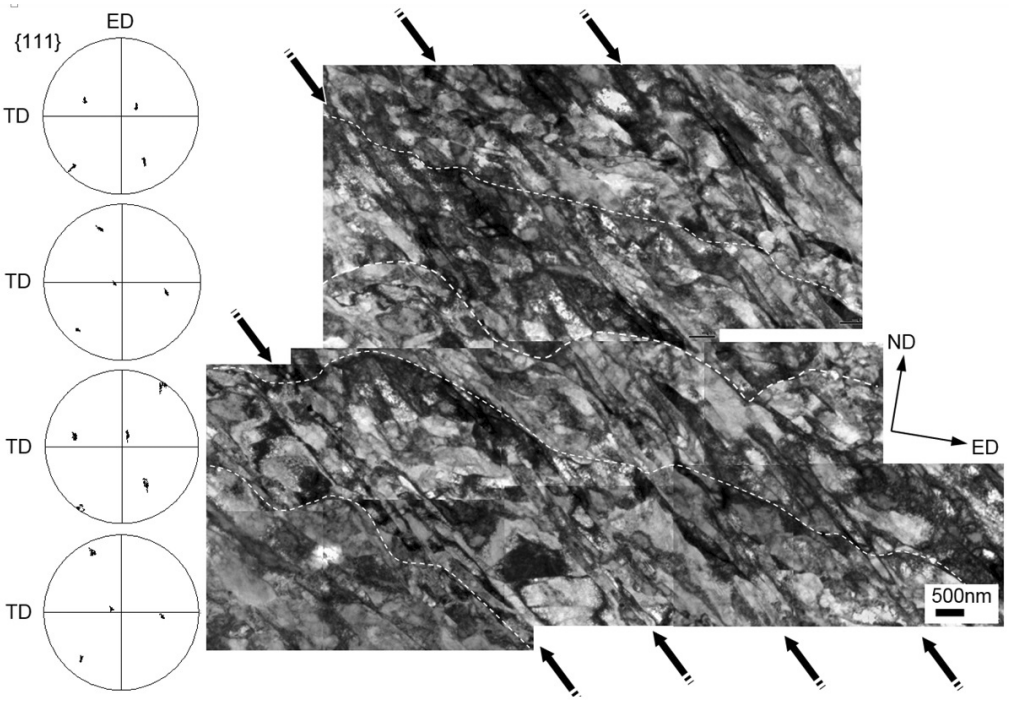

Fig. 5. Microstructure observed inside the area of MSB_1 showing slip propagation across the neighboring grains. The {111} pole figures showing that neighboring grains are nearly complementarily oriented and one of the {111} planes is parallel to the shear plane. Bright field imaging in TEM and TEM local orientation measurements based on Kikuchi patterns

3.1.2. Slip propagation across grain boundaries in coarse-grained copper. SEM/EBSD analysis

The accumulation of SBs into bundles and their propagation through grain boundaries is an important problem in the process of MSBs formation. The sharp crystallographic texture development, observed at increasing deformation, favours the penetration of slip in the macro-shear band area through the neighbouring grains. The situation is simple when neighbouring grains have a similar orientation, and the {111} planes coincide with the plane of maximum shear stress. Slip penetration, however, occurs in regions of quite different orientations. Nevertheless, from the crystallographic point of view, the existence of a common plane for both areas is required; it is along this plane that slip can penetrate the boundary. This was clearly visible within the grains lying inside the MSB, as presented in (Fig. 6).

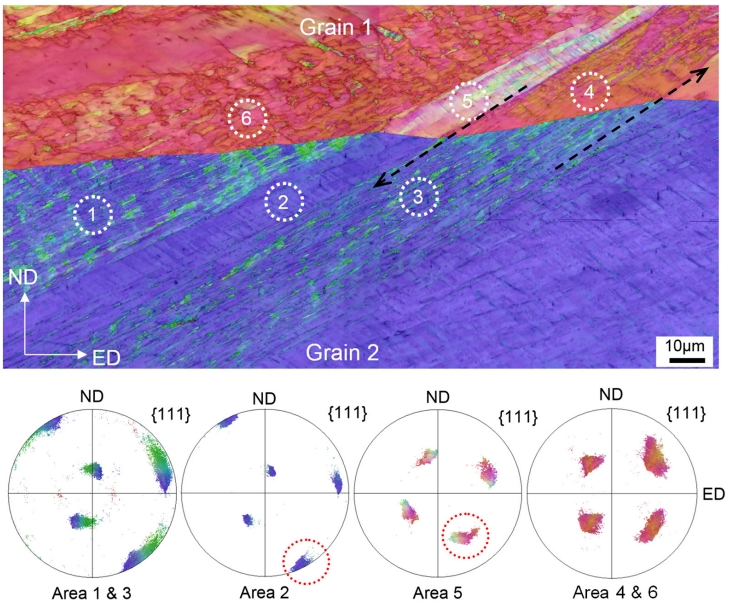

Fig. 6. Slip propagation across boundaries between two neighbouring grains in coarse-grained copper. Orientation map displayed as a 'function' of IPF colour code and corresponding particular areas the {111} pole figures. SEM/EBSD local orientation measurements with step size of 100 nm. Red circles marked the poles of {111} planes important for slip propagation across the grain boundary

Plane strain compression of extremely coarse-grained copper. (Fig. 6) shows the EBSD orientation map displayed as a 'function' of IPF colour code and corresponding particular grains the {111} pole figures from a representative region of localized shear and neighbouring matrix in the copper sample compressed up to 47%. In the longitudinal section, the traces of the {111} planes for both grains were situated (almost) along one line. As a result, characteristic steps are formed on the boundary indicating large shear strains due to localized slip associated with micro- bands. The height of each step in the band direction might be different, depending mainly on the width of the micro-band; the values attain in some cases 1-2 μm. Circles marks in red colour showed the poles of {111} planes important for the slip propagation. It is clear that shear occurred across grain boundaries by the continuity of slip direction although the slip plane (and direction) did not coincide exactly in the adjacent grains. However, an obvious question concerns the way in which the slip propagates across grain boundaries, i.e. whether the stress concentration near the grain boundary leads to slip on {111} plane in <110> directions in the neighbouring grain.

A detailed analysis of the slip traces within all the three grains showed (Fig. 7) that they could be related with the {111} planes. The grain orientations were strongly misoriented. In the longitudinal section the traces of the {111} planes for all pairs of grains were situated (almost) along one line and corresponded to observed traces of the bands. This situation is presented clearly in (Fig. 7), for the boundary between grains 1 and 2 as well as between grains 2 and 3, where the boundaries were penetrated by SB formed compact clusters of two families. Although the traces of bands observed in the longitudinal plane were nearly parallel, in fact the {111} planes, which were important for the analysis in each grain, were slightly misoriented.

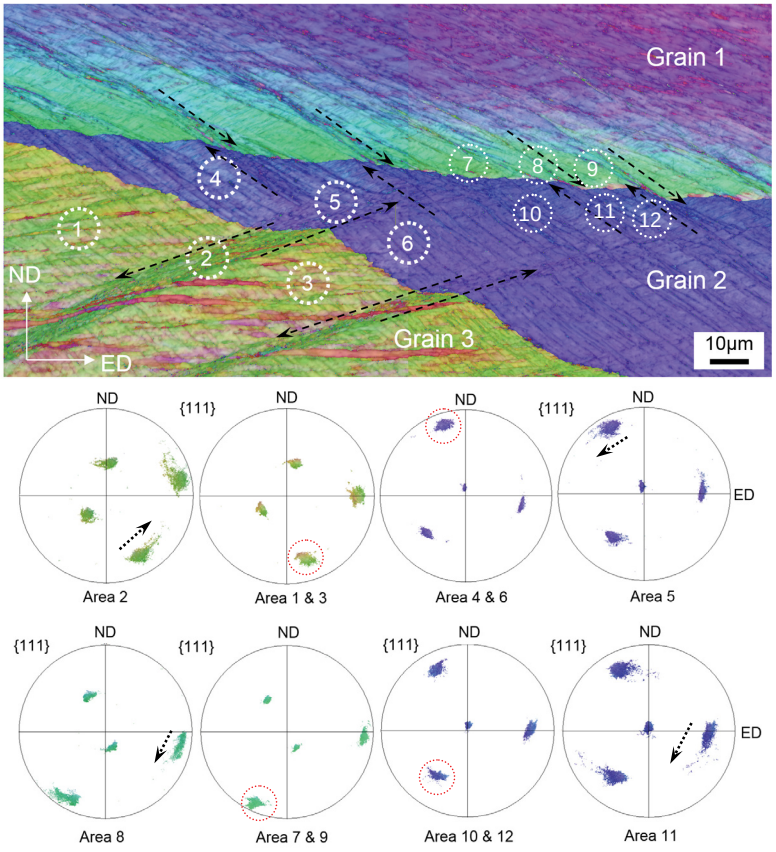

Fig. 7. Slip propagation across the grain boundaries in coarse grained copper. Orientation map displayed as a 'function' of IPF colour code and corresponding particular areas the {111} pole figures. SEM/EBSD local orientation measurements with step size of 100 nm. Red circles marked the poles of {111} planes important for slip propagation across the grain boundary, whereas dotted arrows marked 'direction' of crystal lattice rotation

Rolling. (Fig. 8) shows a number of layers of adjacent elongated grains penetrated by bands of strongly localized strain. It is clearly visible that their crystal lattice rotated in such a way that one of the {111} slip planes became nearly parallel to the direction of maximum shear (their position depends on actual state of anisotropy; in this case is close to 35° to the rolling direction (RD)) although the orientations of some grains were more or less different. Additionally, in each case one of the <011> – type directions, lying in these planes, systematically tended to coincide with shear direction. This leads to the important conclusion that macroscopically observed shear plane in fact consists of small parts limited to particular grains (or their fragments). These parts were only slightly deviated from the macroscopic shear plane. It is important to note that the higher the strain the smaller the deviations from the macro-shear plane. Across these shear bands the crystal orientation changed

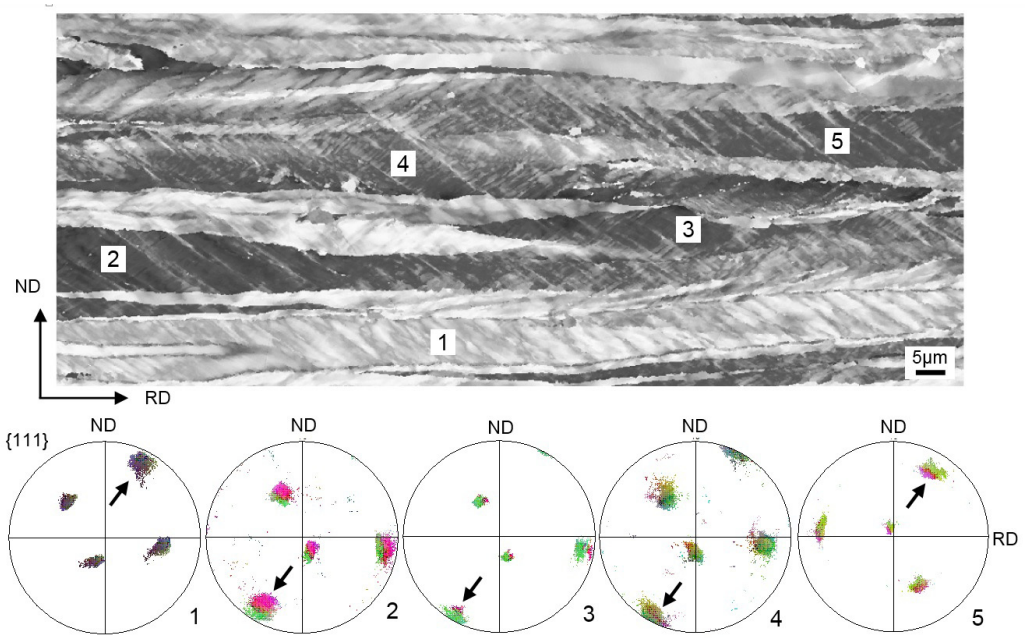

Fig. 8. Microstructure of fine-grained copper deformed ~80% in rolling. (a) Orientation map displayed as a 'function of Schmid factor' in grey scale and the {111} pole figures corresponding particular (marked) grains. SEM-FEG/EBSD local orientation measurements with step size of 100 nm. Black arrows marked important poles of {111} planes

periodically and the accumulated point-to-origin misorientations varied by ~35° but their axes were close to one of the <112> poles, as a 'summary' slip direction of two slips in the <110> directions.

3.2. Macroscopic shear bands in fine-grained AA1050 alloy

3.2.1. Microstructural changes as result of MSB formation

Before PSC the AA1050 alloy possesses a considerable stored energy due to the prior deformation by ECAP and is highly anisotropic. It is expected that PSC, after the change of deformation path, quickly leads to well-defined MSBs and texture changes. The microstructural features of the MSBs were analysed by optical microscopy on re-polished and etched samples. The etching revealed changes in the inclination of the traces of the flat grain boundaries during their incorporation into the MSBs areas.

(Fig. 9a) shows that the traces of the boundaries observed in areas well away from the band are straight and parallel to ED. The very first plastic instability, by which the shear banding began, i.e. the initial distortion of the lamellae within narrow areas, were due to their kinking, as observed in the ND-ED section. This process were initiated near the sample corners, where the grain boundary kinking was the greatest. Near the sample corners, a rigid rotation of the lamellae by ~15-30°, together with their relative translation in the areas outside the band were observed. In the areas near the sample centre, the inclination of the grain boundary traces gradually decreased. This suggests that the MSB propagated from the surfaces in contact with the anvil, near the sample corners, towards the sample centre.

At the MSBs boundary, the traces of boundaries between the flat grains reveal diverse inclinations, varying from 0° to about 30°, to ED, forming transition layers separating the core of the MSB from the matrix, as earlier observed by Hong et al [32] by TEM. The core region of each MSBs is bounded by two transition layers, in which the boundaries between the flat grains are progressively bent. The transition layers have a thickness smaller than or comparable with the core region.

The traces of the grain boundaries revealed a well-defined rotation of opposite sign within each set of bands (Figs. 9). The sense of this rotation is such as to increase the inclination of the layers with respect to ED, i.e. opposite to that of the lamellae which rotate towards the compression plane. (After the ECAP processing, the layers are inclined ~20° to the compression plane, whereas, during PSC, they rapidly align parallel to the compression plane [29]). To a first approximation, the boundaries rotate with respect to the un-sheared areas around an axis close to TD, which is parallel to the shear plane and perpendicular to the shear direction. A comparison between both families of MSBs indicates a clockwise and counter clockwise rotation inside MSB_1 and MSB_2, respectively. This brings the traces of the grain boundaries closer to the shear plane, as observed earlier for twinned structures of different fcc metals, e.g. [17-19,22,23]. The orientation maps measured within the areas of both families of MSBs (Figs. 9b and d) and in the neighbouring matrix (Fig. 9c) confirm the opposite rotations in MSB_1 and MSB_2. Therefore, it is deduced that the textures in the MSB_1 and MSB_2 areas are essentially different.

The orientation maps of MSB_1, MSB_2 and the neighbouring matrix in the ND-TD section revealed that all the layers were

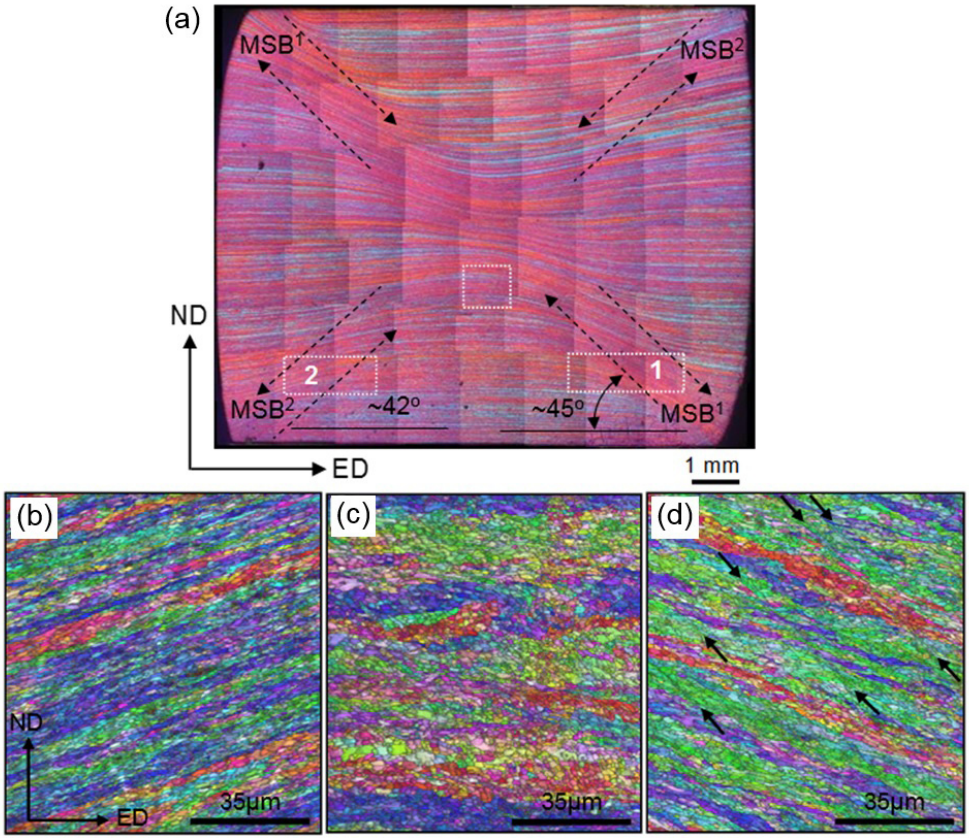

Fig. 9. Macro-shear bands formation during channel-die compression of ECAP processed samples. SEM/EBSD orientation maps showing bending of layers inside MSBs area. Orientation map measured in MSB_1 (b), matrix between bands (c) and MSB_2 (d) areas. Sample pre-deformed in ECAP and then channel-die compressed to logarithmic strains of 0.3. SEM/EBSD local orientation measurements with step size of 100 nm

situated parallel to TD [29]. This confirms again that the most important changes associated with the matrix incorporation into the MSB area were associated with a rigid rotation around axes close to TD.

3.2.2. Strain distribution across and along MSB

The microstructural features of an MSB can be correlated to the measured shear strain and the shear strain gradient in the band. An example of this analysis is shown in (Fig. 10).

The shear strains accumulated in MSB_1 and MSB_2 are different. The maximum shear strain ($\gamma_{max} \sim 0.5$) is observed in the near surface regions of MSB_1, whereas the strain in the same areas of MSB_2 is smaller ($\gamma_{max} \sim 0.3$). A 'line scan' along both MSBs (along the core of the band) shows that the localized strain decreases towards the centre of the sample, as presented in (Fig. 10). This again confirms the thesis that the MSBs are initiated in the near surface areas and propagate towards the sample centre.

Moreover, the highest shear strain values are always associated with the core of the band, where the boundaries of the flat grains were bent to the largest degree, corresponding to the maximum shear strain. Much smaller shear strains are noticed within the transition layers [29]. The maximum shear strain gradients are associated with both 'boundaries' of the core region [29]. An analogous analysis of the lattice rotation in SB has been previously made in pure copper deformed at 77K [18] and at 293K [30], in cold rolled IF-steel [33] and in a Cu-Al alloy [32].

3.2.3. Orientation changes as a result of MSB formation

A detailed investigation of the boundary zone between the matrix and the MSB was carried out on the ND-ED section. The orientation map measured with a step size of 500 nm (to cover a large area) is presented in (Fig. 11a).

For this particular case the map reproduce the microstructure's spatial arrangements and the texture changes near the (MSB_2) / (matrix) boundary zone. Independently of the location (matrix, MSB_1 or MSB_2 area), two groups of orientations were clearly visible, but in quite 'different positions'. To first order, the {111} pole figures measured in the areas of MSB_1 and MSB_2 are positively and negatively rotated around TD, respectively, with respect to the matrix texture. In the band areas, the layers gradually undergo a clockwise (MSB_1) and counter-clockwise (MSB_2) rigid rotation by 30° and 22° around TD, respectively. However, an accurate crystal lattice rotation due to SB formation is more complicated than this rigid body TD rotation.

For particular case of MSB_2 the slip propagation across the grain boundaries is indicated by positions of the {111} planes whose normals have been marked by 'white dotted circles', in (Figs. 11b and c); each circle marks the <111> poles belonging to

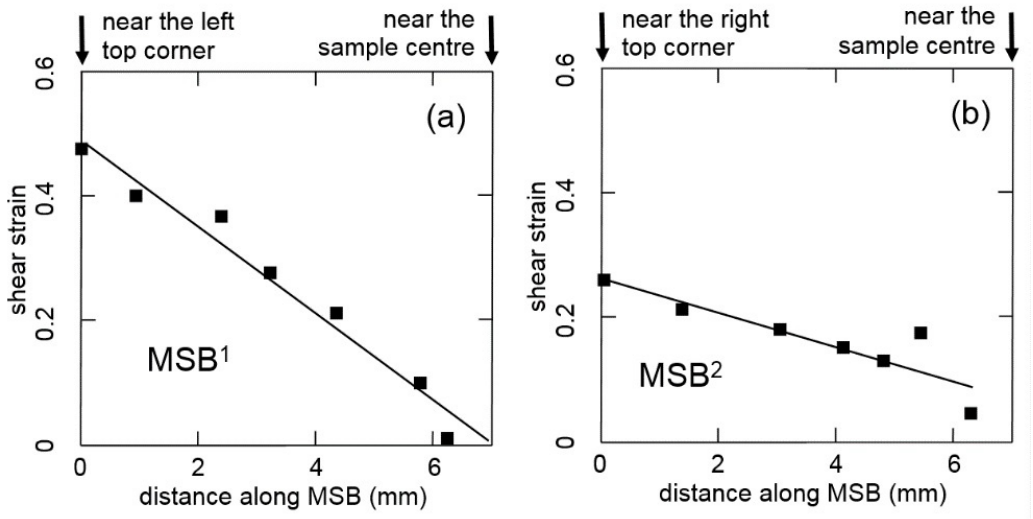

Fig. 10. Distribution of shear strain along MSB_1 (a) and MSB_2 (b). Values from band core [29]

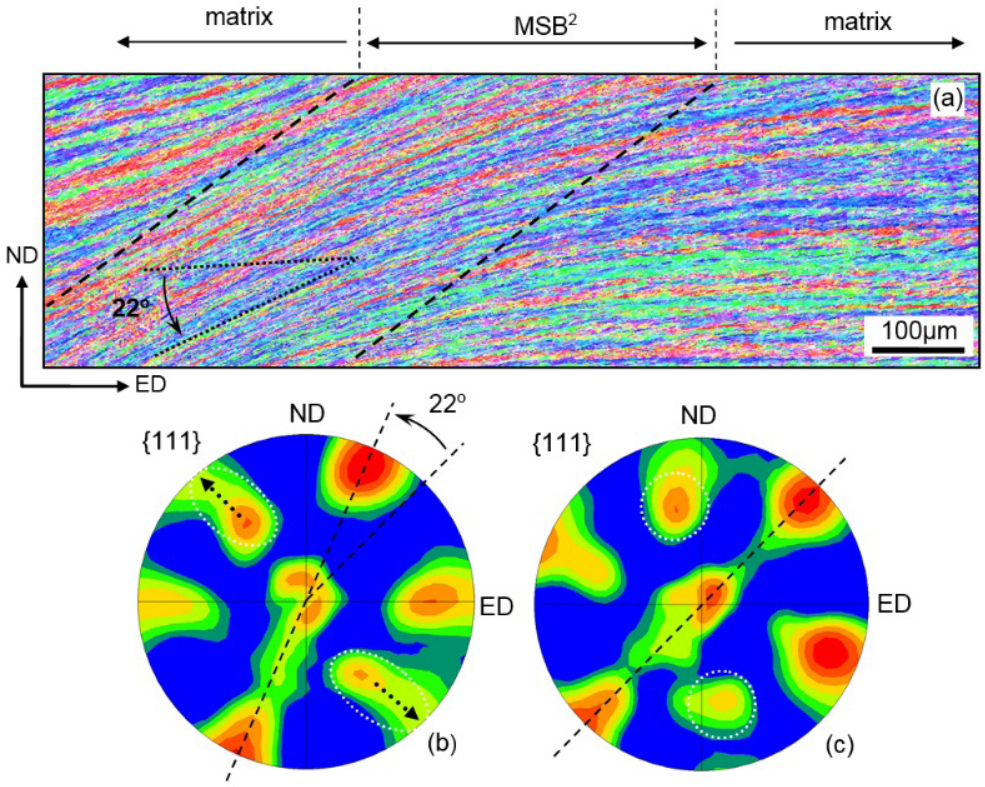

Fig. 11. Orientation changes due to MSB_2 formation. SEM/EBSD orientation map measured in ND-ED plane with step size of 500 nm (a) and corresponding {111} pole figures of MSB_2 (b) and matrix (c) area. IPF (||ED) colour code was applied [29]

one of two groups of orientations. In the matrix area, some of the {111} planes are situated almost parallel to ED, but are inclined by an angle of 10-20° to the compression plane (Fig. 11c). As the matrix is sheared into MSB_2, the orientation map again reveals two types of lattice rotation. The first one (marked by black arrows on (Fig. 11b) is associated with a counter-clockwise rigid body rotation of the MSB_2 texture with respect to the matrix, by an angle of ~22° around TD. The second one (marked by dotted black arrows) is due to the alignment of the particular {111} planes (normals indicated by white dotted circles) parallel to TD.

4. Discussion

4.1. Geometrical description of mechanism of MSB formation

This experimental observation raise important question connected with origin of the local lattice kinking as a precursor to shear band. Some details of this description are based on the approach used in earlier work to explain the local lattice rotation in twinned structures of Cu-Al alloy, e.g. [28]. From geometrical

point of view, the two most important stages of macro-shear banding are shown in an idealized form in (Fig. 12a).

The first step coincides with clockwise (MSB_1) or counter-clockwise (MSB_2) re-orientation of layers within the area of MSB's.

The proposed scenario depicts the sequence of events leading to local kinking of layers, crystal lattice rotation and long distance shear within the band. The first event of this scenario is due to re-grouping of dislocations into low-energy dislocation boundaries, as presented in (Figs. 12b and c). This arrangement of dislocations along the border of 'potential' MSB enables stress relaxation and leads to double lattice kinking with traces inclined at ~ 45° to ED (the inclination depends on the actual state of anisotropy). As a result, the closest {111} planes rotates parallel to the plane of maximum shear (Figs. 12d-e). This increases the Schmid factor of the systems operating on this {111} plane. At the initial stage localized dislocation glide (Figs. 12b and c) on this plane intensifies the rotation tendency within the MSBs. Newly generated dislocations are located at the MSBs border and accommodate increased rotation of the crystal lattice within the band. Finally, as the {111} planes in neighbouring layers are situated parallel to the shear plane long distance slip occurs along the band.

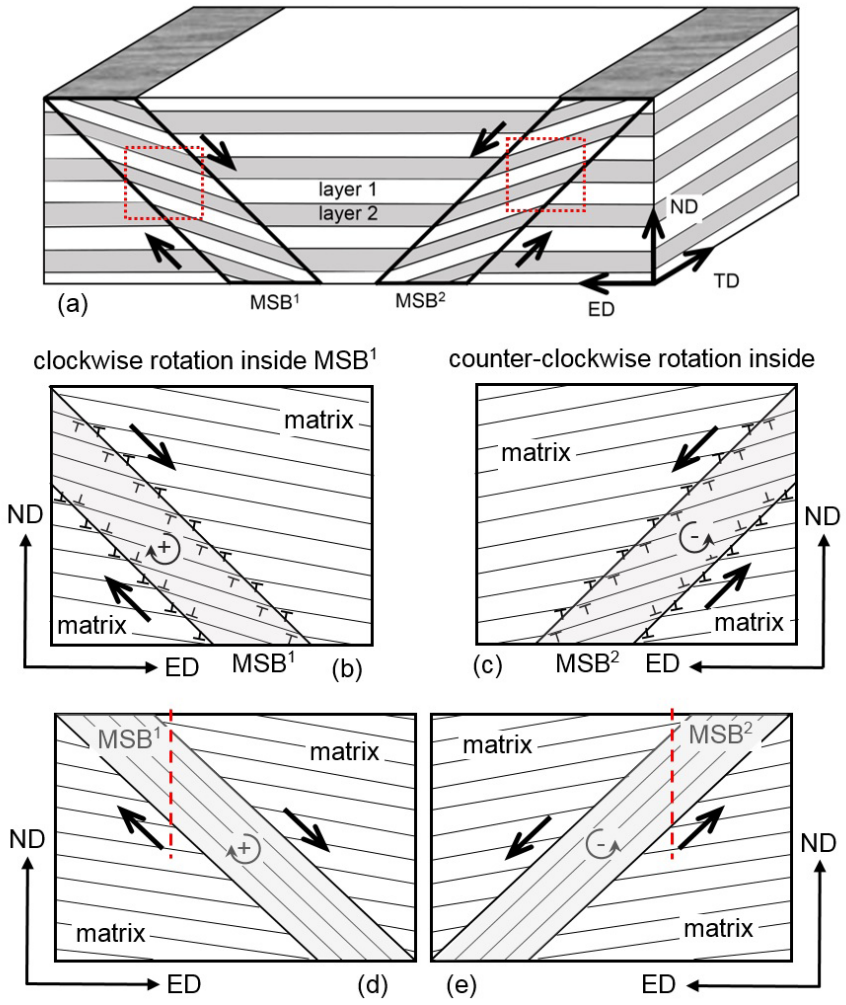

Fig. 12. Schematic presentation of the rotations inside the MSBs. (a) Re-orientation of the structure elements inside MSBs and displacement of the layers outside the bands. (b)-(e) Re-orientation of the traces of {111} planes due to MSBs formation observed in (b)-(e) ND-ED plane. (b), (c) Shear stress induced re-grouping of dislocations into low energy arrangements (short distance dislocation movement) leading to double kinking on the MSB borders and then (d) and (e) long distance movement on re-oriented {111} slip planes inside MSBs [29]

4.2. Local lattice rotation vs. slips organization within macroscopic shear bands

In all analyzed grains lying inside the MSBs a strong tendency to grain subdivision and strain-induced re-orientation was observed. Their crystal lattice rotated in such a way that one of the {111} slip planes became nearly parallel to the direction of the maximum shear. A natural consequence of this rotation is the formation of a specific macro- shear band microtexture which facilitates slip propagation across grain boundaries along the shear direction without any visible variation in the slip direction. The possibility of local re-orientation of the crystal lattice

as a result of SBs formation in single crystals of metals with fcc lattice and low SFE has been demonstrated earlier, e.g. by Paul et al [17-19,22,28].

In the case of complex structure of fine-grained AA1050 alloy two types of boundaries between the grains are observed: the boundaries that separate the grains placed inside a particular layer and the boundaries between grains of adjacent layers. However, always, the rotations occur such that the {111} plane became (nearly) parallel to the shear plane, despite different initial grain orientations. Additionally, one of the <011> – type directions lying in these planes, systematically tends to coincide with the shear direction (Fig. 13).

4.3. Texture components of the copper-type shear bands

The formation of texture components inside copper-type SBs has been discussed in a number of papers, e.g. [7-9, 34]. One hypothesis is that the development of strong shear{100}<011> and minor M{111}<112> components can be related to shear banding [34]. It is clear that the rotation mechanism presented in (Fig. 12) is able to explain the origins of both the near shear{100}<011> orientation and the {111} planes parallel to the shear plane inclined at (+/–) 40-45° to ED. This increases of the slips activity (and stored energy) along shear band plane. However, this is opposite to results of experiments on stored energy [35] carried out for cold rolled aluminum characterized by different texture showed that the amount of stored energy has been found to be much less in the material with shear{100}<011> texture than in that with rolling texture.

In earlier work on C{112}<111> -oriented single crystals of medium-to-high SFE fcc metals deformed in a channel-die, e.g. [7,8,11,17-19], the shear{100}<011> orientation was also observed inside the SBs as a result of a rotation around TD. This always increases the activity of the co-planar slip systems and the intensity of the 'resultant' shear along the <112> direction. In the present work, the shear{100}<011> orientation is only slightly represented at the boundary of scattering. The majority of the grain orientations inside the SBs are rotated from the {100}<011> orientation by ~20° around an axis near the shear plane normal. This leads to the coincidence of the shear direction with the <110> direction. This also indicates that most slip within SBs occurs along the <110> direction but that in some grains of the sheared zone, co-planar slip can take place along a compound <112> direction. However, both cases enable shear (on single or double slip system(s)) along the shear band plane.

The appearance of the M{111}<112> component, can be explained by the tendency to develop certain <111> poles of the matrix, in new positions corresponding to those of the main microtexture components within the MSBs, as suggested in [29]. The rotation mechanism presented in Figs. 11b and c increases the density of the particular <111> poles in the 'areas' of stereographic projection typical of the M{111}<112> orientation. Therefore, the occurrence of the M{111}<112> component inside as shear band can be regarded only as a result of the 'superposition' of selected <111> poles.

This means that shear along the shear band can be observed even when the {111} planes and <110> directions in the grains are slightly deviated from the shear plane and the shear direction, as schematically presented in (Fig. 13). This also leads to the important conclusion that the macroscopically observed shear plane, in fact, consists of small segments limited to the particular grains or their fragments. These parts are only slightly deviated from the macroscopic shear plane). It is important to note that the higher the strain, the smaller the deviation from the MSBs plane (built up of compact clusters of SBs), as concluded earlier in [30].

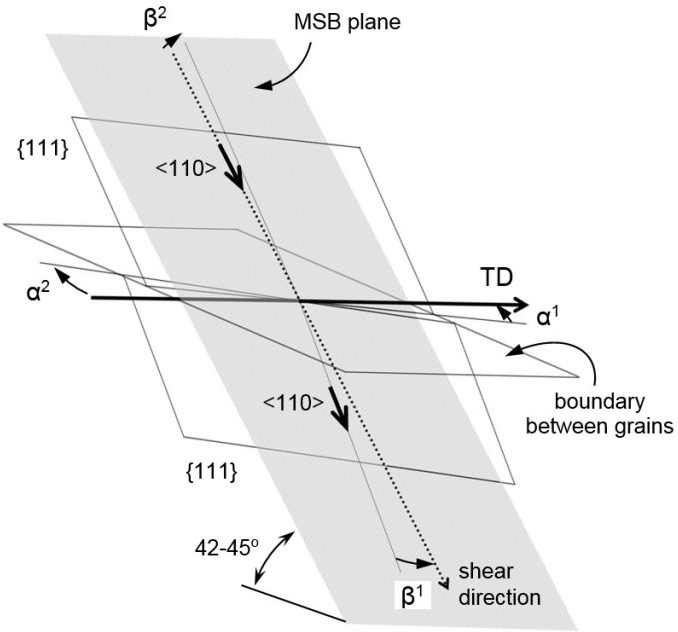

Fig. 13. Shearing along shear band plane in terms of slight misfit between crystal lattices of neighboring areas. {111} planes in grains slightly deviated (by angles of α^1 and α^2) from shear plane, and <110> directions deviated (by angles of β^1 and β^2) from shear direction [29]

5. Conclusions

This study on a coarse- and fine-grained samples of copper and AA1050 alloy clarifies the complex mechanisms responsible for the texture and microstructure evolution resulting from macro- shear bands formation. Microtexture measurements on the samples deformed in terms of plane state of strain, have been used to analyse the slip propagation in the area of macroscopic shear bands. The most important features may be summarized as follows

- They showed that well defined crystal lattice re-orientations occurred in some grains situated within the area of the broad MSBs, although those grains initially had a quite different crystallographic orientations.
- Their crystal lattice rotated in such a way that one of the {111} slip planes became nearly parallel to the direction of maximum shear.

- A natural consequence of this rotation is the formation of specific MSBs texture which facilitates slip propagation across grain boundaries along the shear direction without any visible variation in the slip direction.
- It was thereby established that shear banding occurred across grain boundaries by the continuity of slip direction although the slip plane did not coincide exactly in the adjacent grains.

Acknowledgments

The authors are grateful to Dr A. Tarasek for help in optical metallography and Dr K. Berent for help in SEM/EBSD measurements. This work was supported partially by the National Science Centre (Poland) under grant Number: UMO-2014/13/B/ST8/04291.

REFERENCES

[1] M. Blicharski, S. Gorczyca, Metals Science **12**, 303-312 (1978).
[2] J. Król, B. Major, Bulletin of the Polish Academy of Sciences, Series Technical Sciences **21**, 2255-2263 (1974).
[3] W. Truszkowski, J. Król, B. Major, Bulletin of the Polish Academy of Sciences, Series Technical Sciences **21**, 81-90 (1974).
[4[J. Hirsch, K. Lücke, Acta Metallurgica **36**, 2863-2882 (1988).
[5] C. Donadille, R. Valle, P. Dervin, R. Penelle, Acta Metallurgica **32**, 1547-1565 (1989).
[6] A. Korbel, J.D. Embury, M. Hatherly, P. Martin, Acta Metallurgica **34**, 1999-2009 (1986).
[7] P. Wagner, O. Engler, K. Lücke, Acta Metallurgica et Materialia **43**, 3799-3812 (1995).
[8] Z. Jasieński, T. Baudin, A. Piątkowski, R. Penelle, Scripta Materialia **35**, 397-403 (1996).
[9] H. Paul, M. Darrieulat, A. Piątkowski, Zeitschrift für Metallkunde **11**, 1213-1221 (2001).
[10] A. Duckham, R.D. Knutsen, O. Engler, Acta Materialia **49**, 2739-2749 (2001).
[11] H. Inagaki, M. Koizumi, C.S.T. Chang, B.J. Duggan, Materials Science Forum **587-592**, 396-402 (2002).
[12] J. Król, B. Major, Metals Technology **12**, 477-481 (1979).
[13] W. Truszkowski, J. Król, B. Major, Metal. Transaction A **11A**, 749-758 (1980).
[14] B. Major, Archives of Metallurgy **30**, 279-294 (1985).
[15] W. Truszkowski, J. Król, B. Major, Metallurgical Transaction A **13A**, 665-669 (1982).
[16] T. Leffers, D. Juul Jensen, B. Major, Textures of Materials, 461-467 (1987).
[17] H. Paul, J. H. Driver, C. Maurice, Z. Jasieński, Materials Science Forum A **359**, 178-191 (2003).
[18] H. Paul, A. Morawiec, E. Bouzy, J.J. Fundenberger, A. Piątkowski, Metallurgical and Materials Transactions A **35A**, 3775-3786 (2004).
[19] H. Paul, J.H. Driver, C. Maurice, A. Piątkowski, Acta Materialia **55**, 575-588 (2007).
[20] P. Van Houtte, J.G. Sevillano, E. Aernoudt, Zeitschrift für Metallkunde **70**, 426-432 (1979).
[21] N. Jia, P. Eisenlohr, F. Roters, D. Raabe, X. Zhao, Acta Materialia **60**, 3415-3434 (2012).
[22] H. Paul, C. Maurice, J. H. Driver, Acta Materialia **58**, 2799-2813 (2010).
[23] K. Morii, H. Mecking, Y. Nakayama, Acta Metallurgica & Materialia **33**, 379-386 (1985).
[24] A. Weider, P. Klimanek, Scripta Materialia **38**, 851-856 (1998).
[25] C.S. Da Costa Viana, J.C. Parades, A.L. Pinto, A.M Lopez, [in:] J. Szpunar (Ed.), *Proceeding of the 12th International Conference on Textures of Materials*, Trans Tech Publications, Toronto, Canada, 671-676 (1999).
[26] Y. Nakayama, K. Morii, Transaction of the Japan Institute **23**, 422-431 (1982).
[27] K. Morii, Y. Nakayama, Transaction of the Japan Institute **22**, 857-864 (1981).
[28] H. Paul, A. Morawiec, J.H. Driver, E. Bouzy, International Journal of Plasticity **29**, 1588-1608 (2009).
[29] H. Paul, J.H. Driver, A. Tarasek, W. Wajda, M. Miszczyk, Materials Science and Engineering A **642**, 167-180 (2015).
[30] H. Paul, J.H. Driver, Ceramic Transactions, ed. A. D. Rollett, **201**, 181-188 (2008).
[31] W. Skrotzky, N. Scheerbaum, C.-G. Oertel, H.-G. Brokmeier, S. Suwas, L.S. Toth, Acta Materialia **55**, 2211-2218 (2007).
[32] C.S. Hong, N.R. Tao, X. Huang, K. Lu, Acta Materialia **58**, 3103-3116 (2010) .
[33] Q.Z. Chen, M.Z. Quadir, B.J. Duggan, Philosophical Magazine **86**, 3633-3646 (2006).
[34] Z. Jasienski, J. Pospiech, A. Piatkowski, J. Kusnierz, A. Litwora, K. Pawlik, H. Paul, Material Science Forum **157-162**, 1231-1237 (1994).
[35] B. Major, Texture, Materials Science and Technology **8**, 510-515 (1992).

Received: 20 April 2015.